Neuron, Vol. 37, 765–773, March 6, 2003, Copyright ©2003 by Cell Press

The Sodium-Activated Potassium Channel Is Encoded by a Member of the *Slo* Gene Family

Alex Yuan,[1] Celia M. Santi,[1] Aguan Wei,[1] Zhao-Wen Wang,[1] Kelly Pollak,[1] Michael Nonet,[1] Leonard Kaczmarek,[4] C. Michael Crowder,[2] and Lawrence Salkoff[1,3,*]
[1]Department of Anatomy and Neurobiology
[2]Department of Anesthesiology
[3]Department of Genetics
Washington University School of Medicine
660 S. Euclid Avenue
Saint Louis, Missouri 63110
[4]Department of Pharmacology
Yale University School of Medicine
333 Cedar Street
New Haven, Connecticut 06520

Summary

Na^+-activated potassium channels (K_{Na}) have been identified in cardiomyocytes and neurons where they may provide protection against ischemia. We now report that K_{Na} is encoded by the *rSlo2* gene (also called *Slack*), the mammalian ortholog of *slo-2* in *C. elegans*. *rSlo2*, heterologously expressed, shares many properties of native K_{Na} including activation by intracellular Na^+, high conductance, and prominent subconductance states. In addition to activation by Na^+, we report that rSLO-2 channels are cooperatively activated by intracellular Cl^-, similar to *C. elegans* SLO-2 channels. Since intracellular Na^+ and Cl^- both rise in oxygen-deprived cells, coactivation may more effectively trigger the activity of rSLO-2 channels in ischemia. In *C. elegans,* mutational and physiological analysis revealed that the SLO-2 current is a major component of the delayed rectifier. We demonstrate in *C. elegans* that *slo-2* mutants are hypersensitive to hypoxia, suggesting a conserved role for the *slo-2* gene subfamily.

Introduction

Na^+-activated K^+ channels (K_{Na}) have been reported in guinea pig cardiomyocytes (Kameyama et al., 1984; Luk and Carmeliet, 1990) and various neurons (Bader et al., 1985; Dryer et al., 1989; Dryer, 1991; Schwindt et al., 1989; Egan et al., 1992b; Dale, 1993; Safronov and Vogel, 1996; Bischoff et al., 1998). Native K_{Na} have distinctive properties, including sensitivity to $[Na^+]_i$, a large single channel conductance, subconductance states, and a block of single channel currents at positive potentials, similar to inward rectification.

It is widely accepted that these channels play an important role under ischemic conditions and digitalis toxicity in cardiomyocytes (Kameyama et al., 1984; Luk and Carmeliet, 1990; Mitani and Shattock, 1992). Ischemia causes an increase in $[Na^+]_i$ due primarily to the inhibition of the Na^+/K^+-ATPase. The resulting activation of K_{Na} reduces membrane electrical activity, improves Ca^{2+} transport (preventing intracellular Ca^{2+} accumulation), and may help protect cells by conserving resources under ischemic conditions. In neurons, they may play a similar role (Haddad and Jiang, 1993; Dryer, 1994). In cardiomyocytes, K_{Na} may also be involved in action potential shortening during ischemia (Dryer, 1994). This shortening of the action potential can be mimicked by the application of cardiac glycosides, which inhibit the Na^+/K^+-ATPase, or by the application of K_{ATP} openers. Interestingly, blockade of K_{ATP} channels does not completely abolish the shortening of the action potential, suggesting that K_{ATP} channels are not solely responsible for this effect. Since Na^+ is elevated in ischemic cardiomyocytes, K_{Na} may also contribute to action potential shortening.

In neurons, the role of K_{Na} is more controversial. Since neurons usually have a resting membrane conductance to Na^+ (Nicholls et al., 1992), K_{Na} may be involved in controlling the resting membrane potential. Indeed, in quail trigeminal ganglion neurons, K_{Na} channels are sometimes active at rest (Haimann et al., 1992). They may also serve as a negative feedback mechanism for increased Na^+ channel activity, such as during a train of action potentials, or serve as a conventional delayed rectifier in nonpathological states (Dale, 1993). During a train of action potentials, accumulation of intracellular Na^+ may result in the activation of K_{Na}. It has also been proposed that Na^+ influx through voltage-gated Na^+ channels during an action potential may produce a transient activation of K_{Na}, resulting in action potential repolarization (Bader et al., 1985; Dryer et al., 1989). However, because the sensitivity of native K_{Na} to Na^+ has usually been reported to be very low, the role of K_{Na} in normal cellular physiology is controversial.

Despite the many studies describing K_{Na} in vivo, its molecular identity was unknown. We now show that K_{Na} is encoded by *rSlo2*. *rSlo2* (originally called *Slack*) was recognized as a member of the *Slo* family of K^+ channels when originally cloned (Joiner et al., 1998), but its sensitivity to Na^+ or Cl^- was not tested. *Slo* family channels encode high and intermediate conductance channels sensitive to a variety of intracellular factors. Two other mammalian *Slo* paralogues have been characterized: *Slo1* encodes the BK channel, a Ca^{2+}-activated large conductance K^+ channel (Atkinson et al., 1991; Adelman et al., 1992; Butler et al., 1993), and *Slo3* encodes a pH-sensitive K^+ channel (Schreiber et al., 1998). SLO channels resemble voltage-gated K^+ channels with the addition of a cytoplasmic carboxy-terminal domain. Regions in the carboxy-terminal domain like the RCK domain (Jiang et al., 2001, 2002; Xia et al., 2002) and the "calcium bowl" (Schreiber and Salkoff, 1997; Schreiber et al., 1999) are important for determining ionic sensitivity (Figure 1A). We now show that rSLO-2 is cooperatively activated by Na^+ as well as by Cl^-. Interestingly, the *C. elegans* ortholog *slo-2* is activated by Ca^{2+}/Cl^- rather than Na^+/Cl^- (Yuan et al., 2000). Using mutant analysis in *C. elegans*, we discovered that the SLO-2 current is a major delayed rectifier current in body-wall muscle and that SLO-2 channels protect against hypoxic

*Correspondence: salkoffl@pcg.wustl.edu

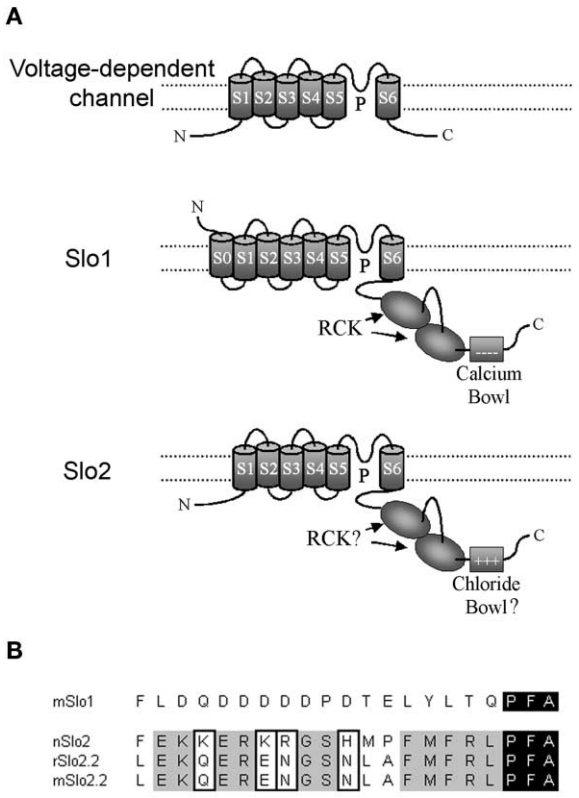

Figure 1. Structural Features of Slo2 Channels

SLO-2 channels are members of the *Slo* gene family of large and intermediate conductance K^+ channels activated by intracellular ions.

(A) Schematic representation comparing the structures of voltage-gated K^+ channels (top), SLO-1 Ca^{2+}- and voltage-activated channels (middle), and SLO-2 channels (bottom). Both SLO-1 and SLO-2 channels resemble voltage-gated K^+ channels but also contain a long cytoplasmic carboxyl terminus domain. In SLO-1 channels, the calcium bowl (Schreiber and Salkoff, 1997; Schreiber et al., 1999) and two predicted RCK domains (Jiang et al., 2002; Xia et al., 2002) are important for sensing intracellular Ca^{2+}. SLO-1 channels also include an additional S0 transmembrane domain (Wallner et al., 1996; Meera et al., 1997). In place of the calcium bowl, SLO-2 channels contain a chloride bowl (Yuan et al., 2000). SLO-2 channels are missing an S0 transmembrane domain.

(B) Sequence alignment in the chloride bowl of SLO-2 channels. Black-shaded residues are identical in all SLO channels. Gray-shaded residues are identical in all SLO-2 channels. Three positions (boxed) in SLO-2 channels are notably different between *C. elegans* SLO-2 (nSlo2) and mammalian SLO-2 (rSlo2.2 and mSlo2.2). The precise locations of the calcium bowl and chloride bowl are shown in Yuan et al., 2000.

death. Together, these results suggest that *Slo2* has evolved to protect against hypoxia by sensing Na^+/Cl^- in mammals and Ca^{2+}/Cl^- in *C. elegans*.

Results

rSlo2 Encodes a Sodium-Activated Potassium Channel

We investigated the properties of rSLO-2 channels in the *Xenopus* oocyte expression system by transcribing cRNA and injecting it into oocytes; the single electrode patch clamp system was used to analyze inside-out patches. Figure 2A, panel i, shows macroscopic currents from an inside-out patch. In the presence of cytoplasmic Na^+, rSLO-2 channels produced large (multi-nanoamp) K^+ currents that showed slight outward rectification over a wide voltage range (−70 mV to +30 mV). No macroscopic channel activity was detected in the absence of $[Na^+]_i$ (Figure 2A, panel ii). Although the current-voltage relationship for rSLO-2 shows slight outward rectification between −70 mV and +30 mV, "inward rectification" is seen at potentials more positive than +30 mV (Figure 2A, panel iii). This phenomenon has been observed in native K_{Na} and may be due to Na^+ block of the outward K^+ current (Wang et al., 1991; Egan et al., 1992b). The activation of macroscopic currents in patches is sharply dependent on the concentration of sodium ion that the cytoplasmic side of the patch is exposed to, with the amplitude of current increasing more than ten times as the sodium concentration is increased from 10 to 50 mM (Figure 2A, panel iv).

Figure 2B shows single channel activity over many seconds; activity dramatically decreased when Na^+_i was removed, but increased upon reintroduction of high Na^+_i. Like K_{Na} channels from native tissue, rSLO-2 channels showed rundown. Channel activity decreased with time, possibly suggesting the wash-out of an intracellular factor required to maintain full channel activity. This rundown phenomenon is observed with inside-out patches of native K_{Na} (Egan et al., 1992b; Dryer, 1993).

Calcium Sensitivity of rSLO-2 Channels

rSLO-2 channels were previously reported as being inhibited by Ca^{2+}_i (Joiner et al., 1998). In that study, rSLO-2 channels were not exposed to Na^+_i, and therefore, the open probability of channels was very low. We confirmed this observation in the absence of Na^+_i, where single channel activity, low to begin with, was further reduced with the addition of 100 μM $[Ca^{2+}]_i$ (data not shown). However, in the presence of 80 mM $[Na^+]_i$, exposure to even higher $[Ca^{2+}]_i$ (200 μM) had no effect on channel activity (data not shown). This is consistent with reports that the native K_{Na} is insensitive to Ca^{2+}_i (Dryer et al., 1989; Haimann et al., 1990, 1992).

Single Channel Properties

Single channel properties of rSLO-2 closely resembled those of native K_{Na}. The single channel conductance of native K_{Na} channels is strongly dependent on K^+_o and K^+_i (Dryer et al., 1989; Haimann et al., 1990; Safronov and Vogel, 1996; Mistry et al., 1997). In one example, native K_{Na} recorded from guinea pig cardiomyocytes had a conductance of 75 pS in symmetrical 60 mM K^+_o/K^+_i and 220 pS in 150/70 mM K^+_o/K^+_i (Mistry et al., 1997). Similarly for rSLO-2, measured conductance changes depending on K^+_o/K^+_i; when the K^+ concentration was increased from symmetrical 80 mM K^+_o/K^+_i to symmetrical 160 mM K^+_o/K^+i, the slope conductance increased from 88 ± 1.8 pS (n = 5) (Figure 3A, panel ii) to 165 ± 6.1 pS (n = 3) (Figure 3B, panel ii). As can be seen from the ramps in both Figures 3A, panel iii, and 3B, panel iii, the single channel conductance significantly rectifies at positive voltages, so the measured single channel

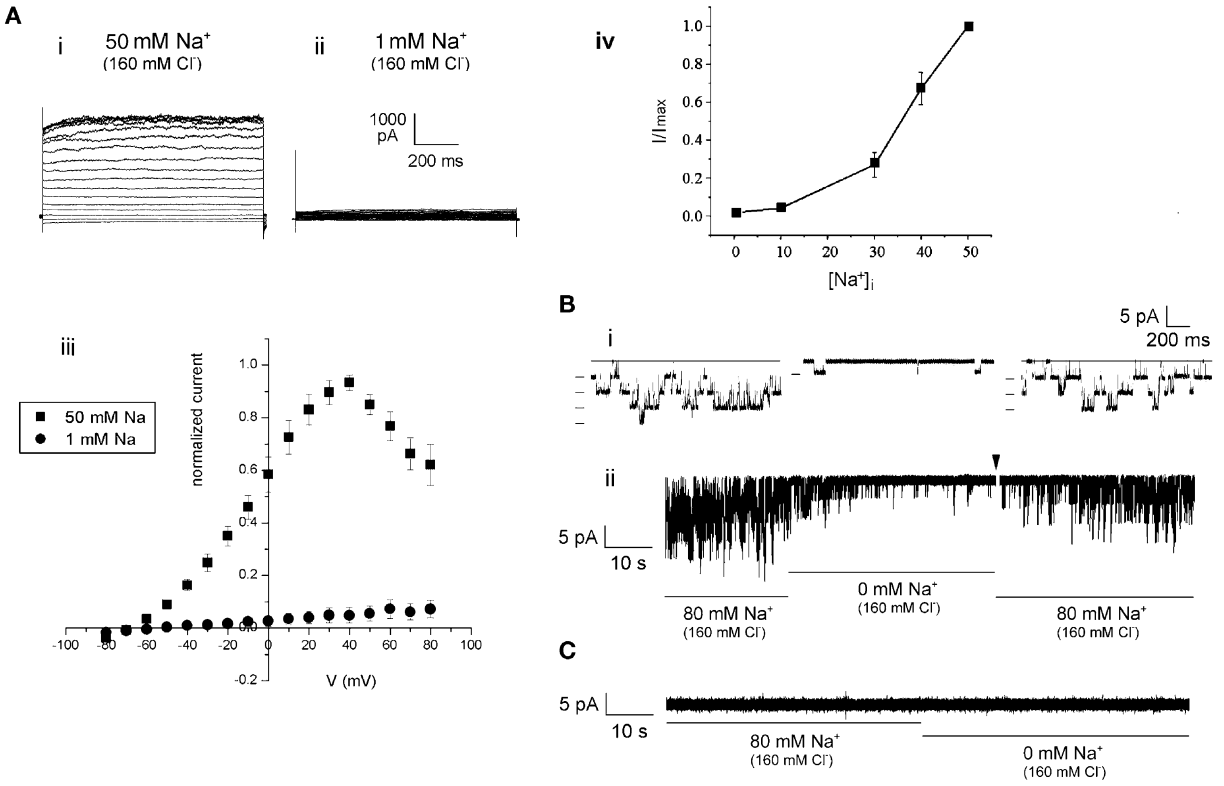

Figure 2. rSLO-2 Is Activated by Sodium

(A) Current traces from an inside-out macropatch (2–3 MΩ electrode prior to seal formation) in the presence of 50 mM $[Na^+]_i$ (i) and in 1 mM $[Na^+]_i$ (ii). Voltage steps (−90 to +70 mV) were applied in 10 mV increments from a holding potential of −70 mV. The calculated potassium equilibrium potential was −78 mV in these experiments. (iii) The current-voltage relationship of the mean current was obtained from seven macropatches with a holding potential of −80 mV, and voltage steps from −80 to +80 mV in 10 mV increments. (iv) Plot of normalized IK_{Na} obtained upon perfusion of inside-out patches with different Na^+ concentrations as indicated.

(B) Single channel currents from an inside-out patch (10 MΩ electrode prior to seal formation) held at −60 mV and perfused with 80 mM $[Na^+]_i$ or 0 mM $[Na^+]_i$ shown on an expanded time scale (i) and a compressed time scale (ii). Four unitary conductance levels can be seen. The arrowhead indicates a gap of ~50 s of data not shown. Symmetric (80 mM) K^+ was used in these experiments.

(C) Current trace of an uninjected oocyte. Although a previous report indicated that endogenous K_{Na} were sparsely present in the membrane of *Xenopus* oocytes (Egan et al., 1992a), recordings from inside-out patches of uninjected oocytes under the conditions we used did not reveal any Na^+-activated K^+ channels (n = 10). On the other hand, most (>90%) of the patches from oocytes injected with *Slo2* cRNA produced multiple channels in high $[Na^+]_i$, and macroscopic currents were observed in a majority of macropatches 3–5 days post injection. For the macropatch experiments, the pipette solution contained (in mM) 145 Na^+-gluconate, 5 KCl, 5 Ca^{2+}-gluconate, 3 Mg^{2+}-gluconate, 11 dextrose, 5 HEPES (pH 7.4) with NaOH. The bath solution contained (in mM): 110 KCl, 50 NaCl, and 5 HEPES (pH 7.3) with KOH. NaCl was replaced by choline-Cl for the dose-response curve. In single channel experiments, the pipette solution contained (in mM) 80 K^+-gluconate, 80 Na^+-gluconate, 5 HEPES, 2 $MgCl_2$ (pH 7.2) with KOH. The bath solution contained (in mM) 80 KCl, 80 NaCl, or 80 choline-Cl, 5 HEPES, 5 EGTA (pH 7.2) with KOH.

conductance varies with the voltage at which it is measured.

Native K_{Na} channels also have prominent subconductance states (Wang et al., 1991), and subconductance states were also observed for rSLO-2 channels (Figures 3A, panel i, and 3B, panels i and iii, arrows). In experiments shown in Figure 3B, panel iii, single channels of approximately 162 pS were observed (at +80 mV) along with single channels with a subconductance level of approximately 50 pS. Single K_{Na} channels are more strongly inwardly rectifying when $K^+_o > K^+_i$ (Luk and Carmeliet, 1990) or when $[Na^+]_i$ is high (Wang et al., 1991; Egan et al., 1992b). The inward rectification of rSLO-2 channels was also weaker in 160 mM K^+_o/K^+_i (Figure 3B, panels ii and iii) compared to 80 mM K^+_o/K^+_i (Figure 3A, panels ii and iii).

Whole Cell Currents

Whole-cell recordings from neurons indicate that $I(K_{Na})$ may be an outwardly rectifying current under physiological conditions (low K^+_o/high K^+_i) (Schwindt et al., 1989; Dale, 1993). We also observed large outward whole cell currents in *rSlo2*-injected oocytes analyzed with the two-electrode voltage clamp technique under physiological conditions (Figure 4A, panel i). These currents closely resembled macroscopic currents from inside-out macropatches using low K^+, high Cl^- external (pipette) solution (Figure 4A, panel ii). In these conditions virtually all macroscopic patch current was outward. Note that E_{Cl} is approximately +87 mV in these experiments. Thus, any contaminating chloride currents would be inward, and virtually no inward current was observed. Whole cell currents from oocytes differed from currents

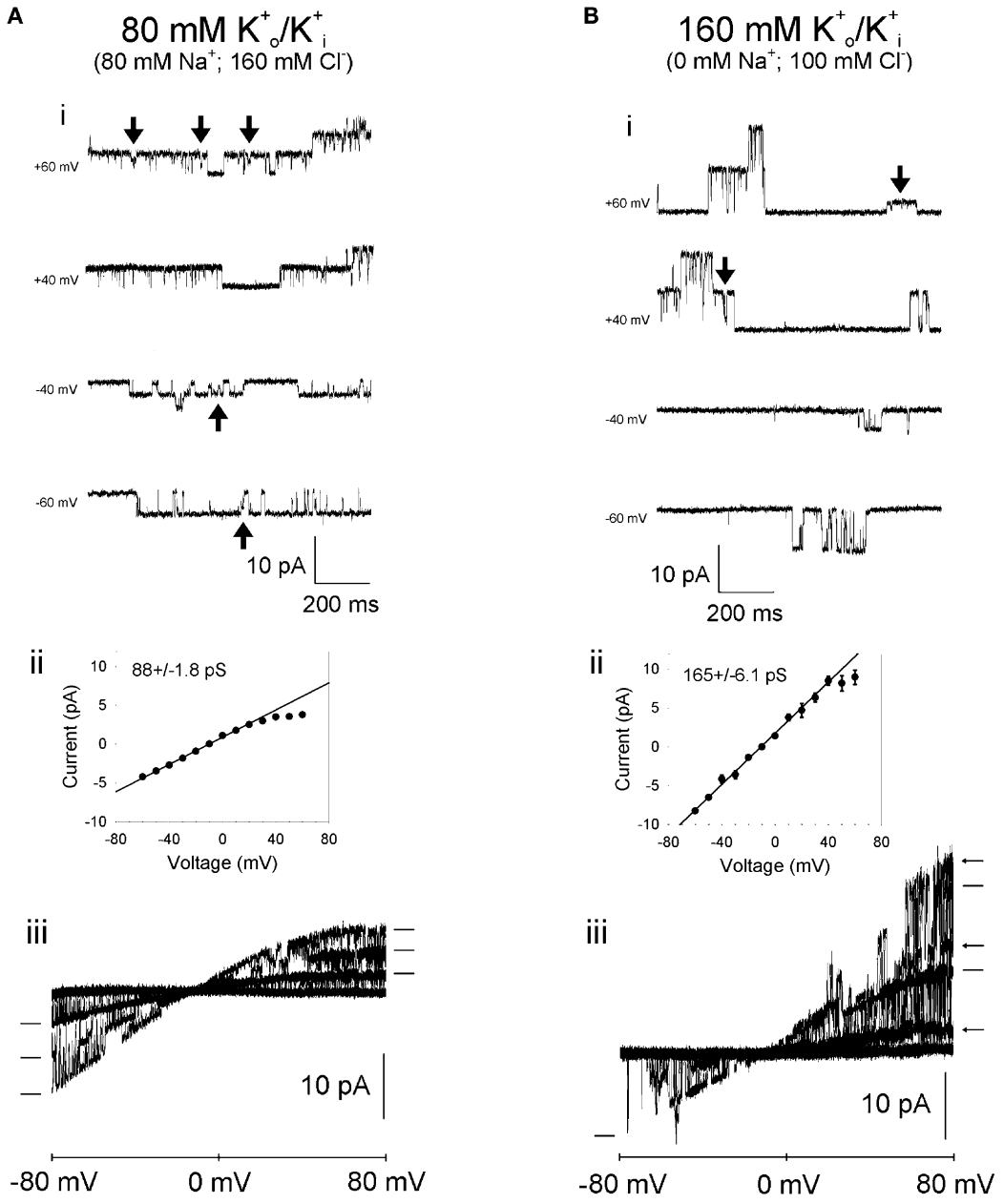

Figure 3. Single rSLO-2 Channels

Single channel conductance of rSLO-2 is dependent on K^+_o and K^+_i.

(A) Single channels recorded from an inside-out patch in 80 mM symmetrical K^+_o/K^+_i. (i) Currents from a patch held at +60, +40, −40, and −60 mV. Arrows indicate subconductance states. (ii) Mean current-voltage relationship of single channels from multiple patches (n = 5). The slope conductance, measured from −60 to +10 mV, is 88 ± 1.8 pS. (iii) Currents evoked by 12 superimposed voltage ramps from −80 to +80 mV. Three main conductance levels are present (horizontal lines). The pipette solution contained (in mM) 80 K^+-gluconate, 80 Na^+-gluconate, 5 HEPES, 2 $MgCl_2$ (pH 7.2) with KOH. The bath solution contained (in mM) 80 KCl, 80 NaCl, 5 HEPES, 5 EGTA (pH 7.2) with KOH.

(B) Single channels recorded from inside-out patches in 160 mM symmetrical K^+_o/K^+_i. (i) Currents from a patch held at +60, +40, −40, and −60 mV. Arrows indicate subconductance states. (ii) Mean current-voltage relationship of single channels from multiple patches (n = 3). The slope conductance, measured from −60 to +10 mV, is 165 ± 6.1 pS. (iii) Currents evoked by 12 superimposed voltage ramps from −80 to +80 mV. Two main conductance levels are present (horizontal lines). Subconductance states of approximately 50 pS (at +80 mV) are indicated by arrows. The pipette solution contained (in mM) 156 K^+-gluconate, 4 KCl, 10 HEPES (pH 7.3) with KOH. The bath solution contained (in mM) 100 KCl, 30 K^+-gluconate, 10 HEPES, 11 EGTA (pH 7.2) with 30 KOH.

seen in macropatches in two respects: a larger percentage of the current showed time dependence of activation (Figure 4A) and whole cell currents lacked the inward rectification or block seen at positive voltages in currents from macropatches (Figure 4B).

Coactivation by Chloride

An unusual property of *slo-2*, the *C. elegans* ortholog of *rSlo2*, is the dependence of the encoded channels on $[Cl^-]_i$ for activation. Hence we tested rSLO-2 channels for $[Cl^-]_i$ dependence and found that they too are acti-

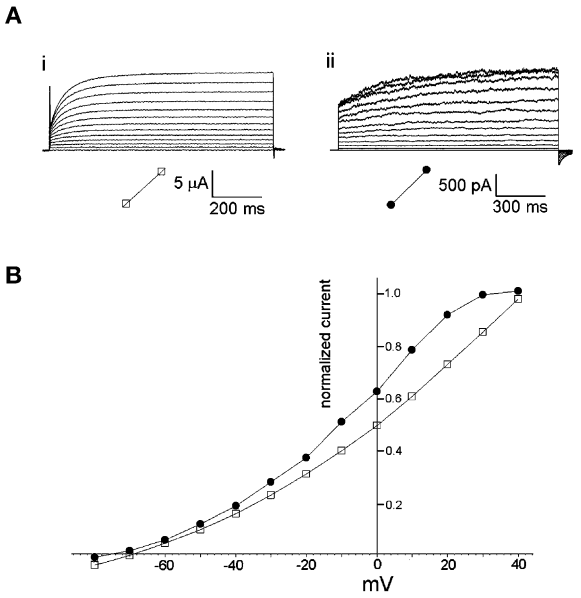

Figure 4. Whole Cell rSLO-2 Currents from Heterologous Expression in *Xenopus* Oocytes Compared with Currents from Macropatches

(A) (i) Current traces from a *Xenopus* oocyte injected with *rSlo2* cRNA and analyzed with the two-electrode voltage clamp method. Approximately 15 μA of outward current was present while uninjected control oocytes expressed less than 100 nA of current. Voltage steps (−80 to +40 mV) were applied in 10 mV increments from a holding potential of −70 mV. Fitting the time-dependent rise of current at +80 mV with a single exponential produced a time constant of approximately 70 ms. Recording pipettes were filled with 3 M KCl, and the oocyte bath solution contained (in mM) 96 NaCl, 2 KCl, 1.8 $CaCl_2$, 1 $MgCl_2$, 5 HEPES (pH 7.5) with NaOH. (ii) Current traces from an inside-out macropatch (2–3 MΩ electrode prior to seal formation) in the presence of 50 mM $[Na^+]_i$. Voltage steps (−80 to +40 mV) were applied in 10 mV increments from a holding potential of −70 mV. Solutions are similar to those used in Figure 2A, panel i.

(B) The normalized current-voltage relationship of the maximal current from the above traces. The currents reversed close to the potassium ion equilibrium potential (−78 mV in macropatch experiments).

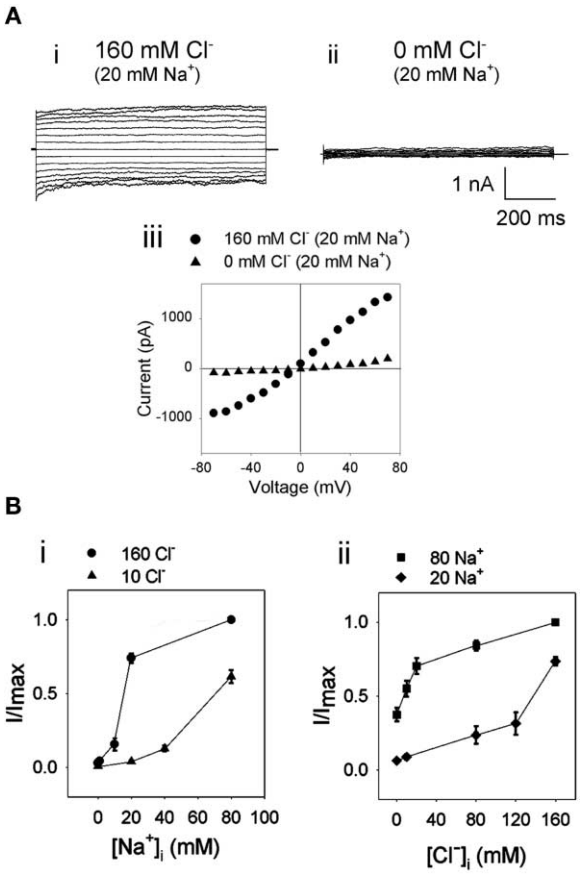

Figure 5. rSLO-2 Is Activated by Chloride

(A) Current traces from an inside-out macropatch (2 MΩ electrode tip) in the presence of 160 mM $[Cl^-]_i$ (i) and in the absence of $[Cl^-]_i$ (ii). Voltage steps (−70 mV to +70 mv) were applied in 10 mV increments from a holding potential of 0 mV. (iii) The current-voltage relationship of the mean current between 700–800 ms. The pipette solution contained (in mM) 80 K^+-gluconate, 80 Na^+-gluconate, 5 HEPES, 2 $MgCl_2$ (pH 7.2) with KOH. The bath solution contained (in mM) 80 KCl or 80 K^+-gluconate, 20 NaCl and 60 choline-Cl or 20 Na^+-gluconate and 120 dextrose, 5 HEPES, 5 EGTA (pH 7.2) with KOH.

(B) (i) Dose-response relationship for $[Na^+]_i$ at 160 mM $[Cl^-]_i$ or 10 mM $[Cl^-]_i$. (ii) Dose-response relationship for $[Cl^-]_i$ at 80 mM $[Na^+]_i$ or 20 mM $[Na^+]_i$. Currents for the dose-response curves were measured and averaged over a 1 s interval at −60 mV, and each patch was normalized to the current elicited in 80 mM $[Na^+]_i$ and 160 mM $[Cl^-]_i$. Each experiment was completed within 120 s to minimize rundown and was perfused in order of decreasing $[Na^+]_i$ or $[Cl^-]_i$.

vated by Cl^-_i (Figure 5A). This activation by Cl^-_i is seen only when Na^+_i is present (Figure 5B, panel i). This is similar to *C. elegans* SLO-2, where Cl^-_i activation is seen only in the presence of Ca^{2+}_i. Notably, *C. elegans* SLO-2 is activated by Ca^{2+}_i and Cl^-_i, instead of Na^+_i and Cl^-_i. This difference in ionic sensitivity between *C. elegans* SLO-2 and rSLO-2 may reflect a relatively greater reliance on voltage-dependent Ca^{2+} channels for inward current in *C. elegans*.

In *C. elegans* SLO-2, the dual requirement for Ca^{2+}_i and Cl^-_i is absolute: no significant macroscopic currents are seen in the absence of either ion (Yuan et al., 2000). In contrast, for rSLO-2, the requirement for Cl^-_i is not absolute; Cl^-_i enhances channel activation, but channels are active at lower levels with Na^+_i alone. This dual activation shows evidence of cooperativity (synergy). That is, the activity of the channel in the presence of both ions is greater than the sum of the activity in either ion alone (Figure 5B, panels i and ii). Such cooperativity could be important in allowing the channel to function in the physiological range of intracellular ion concentrations. Fitting plots with the Hill equation, we found that the $[Na^+_i]_{50}$ was approximately 15 mM with 160 mM $[Cl^-]_i$, but approximately 70 mM with 10 mM $[Cl^-]_i$ (data not shown). The $[Cl_i]_{50}$ was approximately 8.1 mM with 80 mM $[Na^+]_i$, and 131 mM with 20 mM $[Na^+]_i$ (data not shown).

Two Mammalian Slo2 Genes

A search through the mouse genome database revealed a gene (*mSlo2.2*) with a primary amino acid sequence with high similarity to *rSlo2* (96% identity in S1-S6) and is most likely its ortholog. An ortholog of *rSlo2* is also present in the human genome. We determined the tissue distribution of *mSlo2.2* using RT-PCR. *mSlo2.2* was detected in brain, kidney, testis, and faintly in heart (Figure

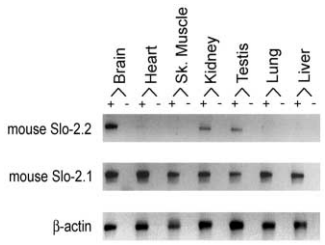

Figure 6. Expression of Two *Slo2* Paralogues in Different Tissues from Mouse

Results from RT-PCR experiments using primers specific for mouse *Slo2.2*, mouse *Slo2.1*, and a β-actin control. Note that *Slo2.2* is the mouse ortholog of *rSlo2*. *Slo2.2* was detected in brain, kidney, and testis. A faint signal was also detected in heart. *Slo2.1* was detected in all tissue types tested. A plus sign indicates the addition of reverse transcriptase to the reaction. A minus sign indicates a control in the absence of reverse transcriptase.

6). A second paralogue (*mSlo2.1*), a more distant relative of *rSlo2*, was also found in the mouse and human genomes. *mSlo2.1* was more widely distributed and was detected in brain, heart, skeletal muscle, kidney, testis, lung, and liver (Figure 6). This data indicates that *mSlo2.2* may be specialized mostly for brain, while *mSlo2.1* may function in broader roles. A newly published study of the distribution of *rSlack* (*rSlo2.2*) in rat brain using an antibody specific to that channel has found the highest intensity of staining in the mitral cells of the olfactory bulb (Bhattacharjee et al., 2002). Significantly, the highest density of K_{Na} channels detected in rat brain by electrophysiology are from the mitral cells of the olfactory bulb (Egan et al., 1992b).

C. elegans SLO-2 Is a Major Current in Muscle

In order to determine what role SLO-2 plays in vivo, we generated two *slo-2* deletion mutants in *C. elegans* (Wei et al., 2002). Using a recently developed *C. elegans* cell culture technique (Christensen et al., 2002), we recorded from wild-type and *slo-2(nf100)* mutant cells in culture. We discovered that currents recorded from muscle cells consisted of two major components, one transient and one delayed. Currents recorded from the *slo-2* mutant had a dramatically reduced delayed component. To quantify the amplitude of the delayed component in wild-type and *slo-2* mutant cells, we measured the current near the end of a 900 ms voltage step in both wild-type and *slo-2* mutants. The average size of the delayed outward current at +60 mV in wild-type cells was 37.6 ± 5 pA/pF (n = 22) compared to 10.0 ± 1 pA/pF (n = 15) in *slo-2* mutant cells. This difference is shown in representative current traces in Figure 7A. In addition to quantitative differences between outward currents in wild-type and *slo-2* mutant cells, there were qualitative differences as well. In 100% of the *slo-2* mutant cells, the transient current was the major outward component (Figure 7A, panel ii). In wild-type cells, single channel openings of a large conductance channel were observed, which resulted in a choppy, high noise level of current traces. However, in the mutant cells, openings of large conductance single channels were never observed and the noise level of current recordings was lower (n =

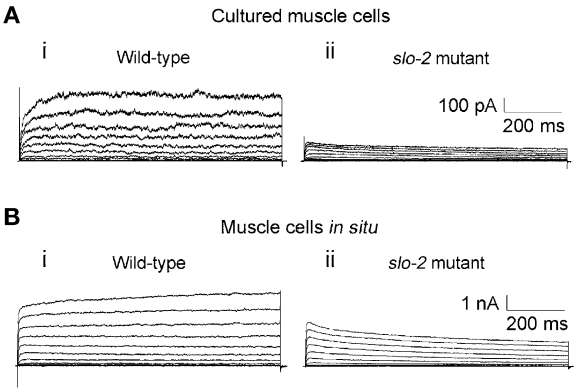

Figure 7. The SLO-2 Current Is the Major Component of the Delayed Rectifier in *C. elegans* Muscle

(A) Current traces from whole-cell patch clamp recordings of wild-type and *slo-2* mutant muscle cells in culture. (i) In most (15/22) wild-type cells, the delayed outward current is larger than the transient current. (ii) In all (15/15) *slo-2(nf100)* mutant cells, the transient current is the larger component. The average delayed current measured between 800 and 900 ms at +60 mV was 37.6 ± 5 pA/pF (n = 22) for wild-type cells, and 10.0 ± 1 pA/pF (n = 15) for mutant cells.
(B) Current traces from whole-cell patch clamp recordings of wild-type and *slo-2* mutant body wall muscle cells recorded in situ from adult animals. (i) In most wild-type cells (4/5), the delayed current is larger than the transient component. (ii) In all (6/6) of the *slo-2(nf100)* mutant cells, the transient current is the larger component. The average delayed current measure between 800 and 900 ms at +60 mV was 130.1 ± 21 pA/pF (n = 5) for wild-type cells, and 48.8 ± 10 pA/pF (n = 6) for mutant cells. Voltage steps (−70 mV to +60 mV) were applied in 10 mV increments with a holding potential of −70 mV. We confirmed these results with two *slo-2* deletion alleles: *slo-2(nf100)* and *slo-2(nf101)* (Wei et al., 2002). The pipette solution contained (in mM) 120 KCl, 20 KOH, 4 $MgCl_2$, 5 Tris, 0.25 $CaCl_2$, 36 sucrose, 5 EGTA, 4 Na_2ATP (pH 7.2) with HCl. The external solution contained (in mM) 140 NaCl, 5 KCl, 5 $CaCl_2$, 5 $MgCl_2$, 11 dextrose, 5 HEPES (pH 7.2) with NaOH.

15). These results suggest that *slo-2* encodes high-conductance channels and that these channels constitute the major component of the delayed outward current in these cells.

Because the cultured muscle cells were embryonic in origin, we confirmed our results in adult body wall muscle cells using the filleted worm prep (Richmond and Jorgensen, 1999; Wang et al., 2001). As in cultured cells, a comparison of adult wild-type and mutant cells showed that the average size of the delayed outward current in wild-type cells was much larger than in mutant cells (130.1 ± 21 pA/pF [n = 5] compared to 48.8 ± 10 pA/pF [n = 6] in mutant cells) (Figure 7B). As with cells in culture, the delayed, noninactivating current was the major component in most wild-type cells (Figure 7B, panel i), but in 100% of mutant *slo-2* cells, the transient current was the major component (Figure 7B, panel ii).

slo-2 Mutants Are Hypersensitive to Hypoxic Death

Mammalian K_{Na} is found in both cardiomyocytes (Kameyama et al., 1984; Luk and Carmeliet, 1990) and neurons (Bader et al., 1985; Dryer et al., 1989; Schwindt et al., 1989; Egan et al., 1992b; Dale, 1993; Safronov and Vogel, 1996; Bischoff et al., 1998), where it may serve a protective role against ischemia by reducing membrane

excitability during hypoxic stress (Kameyama et al., 1984; Dryer, 1994). Since $[Cl^-]_i$ as well as $[Na^+]_i$ and $[Ca^{2+}]_i$ rise during hypoxia (Kameyama et al., 1984; Lai and Nishi, 1998), activation of rSLO-2 by Cl^-_i as well as Na^+_i may boost its ability to sense and react to hypoxic conditions. SLO-2 in *C. elegans* could offer analogous protection against hypoxia by sensing Ca^{2+}_i and Cl^-_i. Using an assay for hypoxic death in *C. elegans* (Scott et al., 2002), we compared the response of wild-type animals to *slo-2* mutants and a mutant of the *slo-1* gene used as a control; *slo-1* encodes a Ca^{2+} but not Cl^--activated K^+ channel (Wang et al., 2001). After a 16 hr incubation in a hypoxic chamber (Experimental Procedures), 58% ± 6% of wild-type animals died, compared to 86% ± 2% of *slo*-2 mutants [both deletion strains combined: 87% ± 2% of *slo-2(nf100)*, 84% ± 3% of *slo-2(nf101)*]. Student's t test showed that *slo-2* mutants were significantly more sensitive to hypoxia than wild-type ($p < 0.001$), whereas a *slo-1* control was not significantly different ($p = 0.818$) (60% ± 6% of *slo-1* [*md1745*]).

Discussion

Role of K_{Na}

A long-standing controversy concerning the role of K_{Na} is the ability of the channel to function under physiological concentrations of Na^+_i. Reports of the Na^+ sensitivity of K_{Na} vary widely, ranging from an EC_{50} of 7.3 to 80 mM (Dryer, 1994). During ischemia or hypoxia, $[Na^+]_i$ increases due to a failure of the Na^+/K^+-ATPase to pump Na^+ out (Kameyama et al., 1984). Since $[Cl^-]_i$ also increases during ischemia, coactivation by both factors, Na^+ and Cl^-, makes it seem more likely that the rSLO-2 channel may be, at least, partially active under conditions of ischemia. Nevertheless, this question has not been settled and requires further investigation. Intracellular chloride is reported to rise to approximately 55 mM in some instances of simulated cardiac ischemia (Lai and Nishi, 1998). Intracellular sodium ion has been reported to range from approximately 19 mM (Nakamura et al., 1999; Kline et al., 1992) to 72 mM (Pogorelov et al., 2002). We undertook experiments within these values in Figure 5, panel ii. From the plot in 20 mM Na^+, we estimate that the current will reach approximately 0.18 of Imax at 55 mM Cl^-. However, a sensitivity to chloride ion has not yet been demonstrated for native sodium-activated potassium channels. In one instance, sodium-activated potassium channels were analyzed in the presence of high levels of chloride, and those channels did not show a particularly high sensitivity to sodium ion (Dryer et al., 1989). Because more than one gene may encode K_{Na} channels, and because other factors such as alternative RNA splicing and accessory subunits may increase the functional heterogeneity of K_{Na} channels, many questions regarding the physiological roles and sodium sensitivity of this intriguing class of channels remain to be investigated.

One point to consider is that, perhaps, only a small number of SLO-2 channels may ever be active, except under the most extreme conditions. The *C. elegans* data shows that SLO-2 represents such a large *potential* outward current in the muscle cells that its complete activation would almost certainly abolish any active inward current response. Conceivably, such a large number of SLO-2 high-conductance channels could furnish a cell with a kind of "safety net" to provide early, "fail-safe" interception and amelioration of the detrimental effects of hypoxia/ischemia, but only a tiny fraction of these channels need be active to respond to the initial effects of hypoxia. A similar mechanism may occur in neurons (Haddad and Jiang, 1993), where *Slo2* may also play a protective role in intercepting the early effects of ischemia. Sodium-activated potassium channels are abundant in many mammalian cells and perhaps act similarly in that usually, only a tiny fraction of this large potential conductance is ever used. Channels held in reserve, which are not usually active, may represent the last line of defense against the more pathological conditions that accompany ischemia, namely a rise in the bulk concentrations of intracellular ions that can lead to a fatal osmotic imbalance.

Mechanism of Na^+/Cl^--Activation

The activation of rSLO-2 by Na^+ and its *C. elegans* ortholog by Ca^{2+} poses an interesting question. What is the mechanism of Ca^{2+}/Cl^- or Na^+/Cl^- sensing? Site-directed mutagenesis previously showed that a region in the tail of the *C. elegans* SLO-2 channel ("chloride bowl") is important for sensing Ca^{2+}_i and Cl^-_i (Yuan et al., 2000), and the "calcium bowl," an analogous region in the BK (SLO-1) channel, is important for sensing $[Ca^{2+}]_i$ (Schreiber and Salkoff, 1997; Schreiber et al., 1999). The calcium bowl consists of a string of negatively charged amino acid residues that are perfectly conserved in all SLO-1 channels. These negative charges may help to coordinate Ca^{2+} in SLO-1 channels. In contrast, the chloride bowl consists of a string of positively charged residues in many positions that correspond to negative charges in the calcium bowl (Figure 1B). Whether these residues help coordinate Cl^- and perhaps even cooperatively bind Ca^{2+} remains to be determined. Nevertheless, site-directed changes in the chloride bowl produced one mutant that significantly reduced sensitivity of gating to both Ca^{2+} and Cl^- and another mutant that eliminated sensitivity to Ca^{2+} and Cl^- altogether (Yuan et al., 2000). Hence, differences in the amino acid sequence between the mammalian and *C. elegans* SLO-2 channels in this region may conceivably relate to differences between *C. elegans* SLO-2 and rSLO-2 with respect to Ca^{2+}/Cl^- versus Na^+/Cl^- activation (Figure 1B).

In Slo1 channels, a second region possibly corresponding to a RCK domain (Jiang et al., 2001, 2002) has recently been discovered to also be important for sensing Ca^{2+} (Jiang et al., 2001, 2002; Xia et al., 2002). Conceivably, one or more RCK domains are also present in Slo2 at corresponding sites. Such regions might also be important for determining the gating properties in *C. elegans* and mammalian SLO-2 channels.

Evolution of a Na^+/Cl^--Activated Channel

The difference in ion dependence of gating between the SLO-2 orthologs in *C. elegans* and mammals may reflect a relatively more important role that Ca^{2+} plays in *C. elegans* since a voltage-gated Na^+ channel is apparently

absent (Bargmann, 1998). It has been suggested that Ca^{2+} channels may have preceded Na^+ channels in evolution (Hille, 1992). Perhaps a Ca^{2+}/Cl^--activated Slo channel was present in a common ancestor to *C. elegans* and vertebrates. Following the evolution of Na^+ channels and its rise to prominence in carrying inward current, this ancestral Slo channel may have evolved to sense Na^+/Cl^- instead of Ca^{2+}/Cl^-.

Protection against Hypoxia May Be a Conserved Role

Using a hypoxic death assay, *slo-2* mutants showed hypersensitivity to hypoxic death, suggesting that *slo-2* in *C. elegans* protects against the detrimental effects of hypoxia. During hypoxia, an increase in intracellular Na^+ is followed by an increase in intracellular Ca^{2+} and Cl^-. A possible scenario is that in mammals, the rise in Na^+/Cl^- activates SLO-2 channels, while in *C. elegans*, the rise in Ca^{2+}/Cl^- causes activation. The resulting activation of SLO-2 may protect the cell by hyperpolarizing the resting potential, limiting electrical activity, and improving Ca^{2+} transport.

Clinical Relevance

The identification of the molecular identity of K_{Na} will allow for the development of specific agonists and antagonists. New therapies might be developed for treatment of any condition involving hypoxia including angina, stroke, cardiac ischemia, cardiac arrhythmias, brain trauma, fetal hypoxia, and hypoxia during organ transplantation. In this latter role, preconditioning organs for transplant using K_{ATP} channel openers now appears to be highly effective (Zhang et al., 2001). Indeed, hypoxic preconditioning may prove to be the key to success in many operations involving brain and heart. Because sodium-activated potassium channels are widespread, openers for this channel may be equally or more effective than openers for K_{ATP} in clinical medicine.

Experimental Procedures

Xenopus Oocyte Expression

In order to obtain efficient expression of *rSlo2* in *Xenopus* oocytes, we cloned the original *rSlo2* construct into pOX, a vector we optimized for oocyte expression. Capped cRNA was synthesized using the T3 mMessage mMachine kit (Ambion). *rSlo2* was linearized using NotI. cRNA reactions were resuspended in nuclease-free water to a final concentration of 1.5 μg/μl. Oocytes were harvested from adult female *Xenopus laevis* as described (Yuan et al., 2000). Defolliculated oocytes were injected with approximately 75 ng of cRNA using a Drummond Nanojector. Injected oocytes were incubated at 19°C in ND96 medium (in mM): 96 NaCl, 2 KCl, 1.8 $CaCl_2$, 1 $MgCl_2$, 5 HEPES (pH 7.5) with NaOH. Oocytes were analyzed 2–3 days after injection for single channel analysis, or 3–6 days after injection for macroscopic current analysis.

Electrophysiology

Prior to recording, the vitelline membranes were mechanically removed. The contents of solutions used are described in the figure legends. Traces were acquired using an Axopatch 200A (Axon Instruments), digitized at 10 kHz and filtered at 2 kHz. Data were analyzed using pClamp 8.2 (Axon Instruments) and Sigmaplot 5 (Jandel Scientific) or Origin 6.0 (Microcal).

RT-PCR

First strand synthesis was performed with PowerScript™ reverse transcriptase (Clonetech) for each tissue with 5.0 μg total RNA, primed with 5.0 μM random hexanucleotides, incubated with 250 μM dNTPs at 42°C for 1 hr. Five percent of each first strand reaction was assayed by PCR using 0.5 μM oligonucleotides, 200 μM dNTPs, and 1.0 unit of *Taq* DNA polymerase and cycled 35 times. Reaction products were electrophoresed on 2% agarose gels, using Tris borate (TBE) buffer and visualized with ethidium bromide. Sequence of PCR primer pairs and cycling conditions available upon request.

Cell Culture

Embryonic cells were isolated and cultured as described in Christensen et al. (2002) with the following modifications. Nematode eggs were not separated from adult carcasses in a sucrose gradient. Cellular debris and carcasses were removed upon filtration. Muscle cells were identified based on their distinctive morphology in cell culture. An integrated *myo-3*::GFP transformed strain, which labeled the body wall muscle cells with GFP, verified the method of identification (Christensen et al., 2002).

In Situ Muscle Recordings

Adult nematodes were filleted and prepared for single electrode whole-cell recording of body wall muscle as previously described (Richmond and Jorgensen, 1999; Wang et al., 2001).

Hypoxia Assay

Synchronous unstarved NGM agar cultures of adult *C. elegans*, two days post L4 stage, were transferred with 1 ml M9 to 1.5 ml polypropylene tubes and were placed in the hypoxia chamber (Forma Scientific, model #1025) filled with anoxic gas (5% CO_2, 10% H_2, 85% N_2) and maintained at 27°C. The M9 was replaced three times with 1 ml of M9 (that had been vigorously bubbled for 30 min with anoxic gas) with the final wash removed to leave the animals in 100 μl. Oxygen tension in the hypoxia chamber was $<0.2\%$ as measured by an O_2 meter and electrode (Microelectrodes, Inc.; OM4 meter, MI730 electrode). After the hypoxic incubation period, the animals were transferred back to agar plates and allowed to recover in room air for 24 hr before scoring for spontaneous or evoked movement (touching with a platinum wire). Animals not moving were scored as dead (as a control experiment, we determined that 0% of wild-type and mutant animals (*nf100*) died with a similar incubation in atmospheric O_2). Student's t test was used to assess statistical significance. There was no significant change in pH in these experiments. The buffer used in the *slo-2* hypoxia experiments was M9. M9 is a modified phosphate-buffered saline, 86 mM NaCl, 42 mM Na_2HPO_4, 22 mM KH_2PO_4, 1 mM $MgSO_4$ (pH 6.98–7.02). Deoxygenating M9 with the hydrogen, nitrogen, CO_2 mixture results in a negligible drop in pH of 0.01–0.05 units to 6.97.

Acknowledgments

Supported by grants from the NIH to L.S. and the Washington University McDonnell Center for Cellular and Molecular Neurobiology. We also thank Bill Joiner, Alice Butler, and Gloria Fawcett for help and advice.

Received: October 15, 2002
Revised: January 21, 2003

References

Adelman, J.P., Shen, K.Z., Kavanaugh, M.P., Warren, R.A., Wu, Y.N., Lagrutta, A., Bond, C.T., and North, R.A. (1992). Calcium-activated potassium channels expressed from cloned complementary DNAs. Neuron *9*, 209–216.

Atkinson, N.S., Robertson, G.A., and Ganetzky, B. (1991). A component of calcium-activated potassium channels encoded by the *Drosophila* slo locus. Science *253*, 551–555.

Bader, C.R., Bernheim, L., and Bertrand, D. (1985). Sodium-activated potassium current in cultured avian neurones. Nature *317*, 540–542.

Bargmann, C.I. (1998). Neurobiology of the *Caenorhabditis elegans* genome. Science *282*, 2028–2033.

Bhattacharjee, A., Gan, L., and Kaczmarek, L.K. (2002). Localization of the Slack potassium channel in the rat central nervous system. J. Comp. Neurol. *454*, 241–254.

Bischoff, U., Vogel, W., and Safronov, B.V. (1998). Na^+-activated K^+ channels in small dorsal root ganglion neurones of rat. J. Physiol. *510*, 743–754.

Butler, A., Tsunoda, S., McCobb, D.P., Wei, A., and Salkoff, L. (1993). mSlo, a complex mouse gene encoding "maxi" calcium-activated potassium channels. Science *261*, 221–224.

Christensen, M., Estevez, A., Yin, X., Fox, R., Morrison, R., McDonnell, M., Gleason, C., Miller, D.M., 3rd, and Strange, K. (2002). A primary culture system for functional analysis of *C. elegans* neurons and muscle cells. Neuron *33*, 503–514.

Dale, N. (1993). A large, sustained Na(+)- and voltage-dependent K+ current in spinal neurons of the frog embryo. J. Physiol. *462*, 349–372.

Dryer, S.E. (1991). Na(+)-activated K+ channels and voltage-evoked ionic currents in brain stem and parasympathetic neurones of the chick. J. Physiol. *435*, 513–532.

Dryer, S.E. (1993). Properties of single Na(+)-activated K+ channels in cultured central neurons of the chick embryo. Neurosci. Lett. *149*, 133–136.

Dryer, S.E. (1994). Na(+)-activated K+ channels: a new family of large-conductance ion channels. Trends Neurosci. *17*, 155–160.

Dryer, S.E., Fujii, J.T., and Martin, A.R. (1989). A Na^+-activated K^+ current in cultured brain stem neurones from chicks. J. Physiol. *410*, 283–296.

Egan, T.M., Dagan, D., Kupper, J., and Levitan, I.B. (1992a). Na(+)-activated K+ channels are widely distributed in rat CNS and in *Xenopus* oocytes. Brain Res. *584*, 319–321.

Egan, T.M., Dagan, D., Kupper, J., and Levitan, I.B. (1992b). Properties and rundown of sodium-activated potassium channels in rat olfactory bulb neurons. J. Neurosci. *12*, 1964–1976.

Haddad, G.G., and Jiang, C. (1993). O_2 deprivation in the central nervous system: on mechanisms of neuronal response, differential sensitivity and injury. Prog. Neurobiol. *40*, 277–318.

Haimann, C., Bernheim, L., Bertrand, D., and Bader, C.R. (1990). Potassium current activated by intracellular sodium in quail trigeminal ganglion neurons. J. Gen. Physiol. *95*, 961–979.

Haimann, C., Magistretti, J., and Pozzi, B. (1992). Sodium-activated potassium current in sensory neurons: a comparison of cell-attached and cell-free single-channel activities. Pflugers Arch. *422*, 287–294.

Hille, B. (1992). Ion Channels of Excitable Membranes (Sunderland, MA: Sinauer Associates).

Jiang, Y., Pico, A., Cadene, M., Chait, B.T., and MacKinnon, R. (2001). Structure of the RCK domain from the *E. coli* K^+ channel and demonstration of its presence in the human BK channel. Neuron *29*, 593–601.

Jiang, Y., Lee, A., Chen, J., Cadene, M., Chait, B.T., and MacKinnon, R. (2002). Crystal structure and mechanism of a calcium-gated potassium channel. Nature *417*, 515–522.

Joiner, W.J., Tang, M.D., Wang, L.Y., Dworetzky, S.I., Boissard, C.G., Gan, L., Gribkoff, V.K., and Kaczmarek, L.K. (1998). Formation of intermediate-conductance calcium-activated potassium channels by interaction of Slack and Slo subunits. Nat. Neurosci. *1*, 462–469.

Kameyama, M., Kakei, M., Sato, R., Shibasaki, T., Matsuda, H., and Irisawa, H. (1984). Intracellular Na^+ activates a K^+ channel in mammalian cardiac cells. Nature *309*, 354–356.

Kline, R.P., Hanna, M.S., Dresdner, K.P., Jr., and Wit, A.L. (1992). Time course of changes in intracellular K^+, Na^+, and pH of subendocardial Purkinje cells during the first 24 hours after coronary occlusion. Circ. Res. *70*, 566–575.

Lai, Z.F., and Nishi, K. (1998). Intracellular chloride activity increases in guinea pig ventricular muscle during simulated ischemia. Am. J. Physiol. *275*, H1613–H1619.

Luk, H.N., and Carmeliet, E. (1990). Na(+)-activated K+ current in cardiac cells: rectification, open probability, block and role in digitalis toxicity. Pflugers Arch. *416*, 766–768.

Meera, P., Wallner, M., Song, M., and Toro, L. (1997). Large conductance voltage- and calcium-dependent K^+ channel, a distinct member of voltage-dependent ion channels with seven N-terminal transmembrane segments (S0–S6), an extracellular N terminus, and an intracellular (S9–S10) C terminus. Proc. Natl. Acad. Sci. USA *94*, 14066–14071.

Mistry, D.K., Tripathi, O., and Chapman, R.A. (1997). Kinetic properties of unitary Na^+-dependent K^+ channels in inside-out patches from isolated guinea-pig ventricular myocytes. J. Physiol. *500*, 39–50.

Mitani, A., and Shattock, M.J. (1992). Role of Na-activated K channel, Na-K-Cl cotransport, and Na-K pump in [K]e changes during ischemia in rat heart. Am. J. Physiol. *263*, H333–H340.

Nakamura, T., Hayashi, H., Satoh, H., Katoh, H., Kaneko, M., and Terada, H. (1999). A single cell model of myocardial reperfusion injury: changes in intracellular Na^+ and Ca^{2+} concentrations in guinea pig ventricular myocytes. Mol. Cell. Biochem. *194*, 147–157.

Nicholls, J.G., Martin, A.R., and Wallace, B.G. (1992). From Neuron to Brain (Sunderland, MA: Sinauer Associates).

Pogorelov, A.G., Pogorelova, V.N., Dubrovkin, M.I., Demin, I.P., and Khrenova, E.V. (2002) Activation of specific membrane mechanisms in the myocardium cells on early stages of ischemia. Biofizika *47*, 744–751.

Richmond, J.E., and Jorgensen, E.M. (1999). One GABA and two acetylcholine receptors function at the *C. elegans* neuromuscular junction. Nat. Neurosci. *2*, 791–797.

Safronov, B.V., and Vogel, W. (1996). Properties and functions of Na(+)-activated K+ channels in the soma of rat motoneurones. J. Physiol. *497*, 727–734.

Schreiber, M., and Salkoff, L. (1997). A novel calcium-sensing domain in the BK channel. Biophys. J. *73*, 1355–1363.

Schreiber, M., Wei, A., Yuan, A., Gaut, J., Saito, M., and Salkoff, L. (1998). Slo3, a novel pH-sensitive K^+ channel from mammalian spermatocytes. J. Biol. Chem. *273*, 3509–3516.

Schreiber, M., Yuan, A., and Salkoff, L. (1999). Transplantable sites confer calcium sensitivity to BK channels. Nat. Neurosci. *2*, 416–421.

Schwindt, P.C., Spain, W.J., and Crill, W.E. (1989). Long-lasting reduction of excitability by a sodium-dependent potassium current in cat neocortical neurons. J. Neurophysiol. *61*, 233–244.

Scott, B.A., Avidan, M.S., and Crowder, C.M. (2002). Regulation of hypoxic death in *C. elegans* by the insulin/IGF receptor homolog DAF-2. Science *296*, 2388–2391.

Wallner, M., Meera, P., and Toro, L. (1996). Determinant for beta-subunit regulation in high-conductance voltage-activated and Ca(2+)-sensitive K+ channels: an additional transmembrane region at the N terminus. Proc. Natl. Acad. Sci. USA *93*, 14922–14927.

Wang, Z., Kimitsuki, T., and Noma, A. (1991). Conductance properties of the Na(+)-activated K+ channel in guinea-pig ventricular cells. J. Physiol. *433*, 241–257.

Wang, Z.W., Saifee, O., Nonet, M.L., and Salkoff, L. (2001). SLO-1 potassium channels control quantal content of neurotransmitter release at the *C. elegans* neuromuscular junction. Neuron *32*, 867–881.

Wei, A., Yuan, A., Fawcett, G., Butler, A., Davis, T., Xu, S.-Y., and Salkoff, L. (2002). Efficient isolation of targeted *Caenorhabditis elegans* deletion strains using highly thermostable restriction endonucleases and PCR. Nucleic Acids Res. *30*, e110.

Xia, X.M., Zeng, X., and Lingle, C.J. (2002). Multiple regulatory sites in large-conductance calcium-activated potassium channels. Nature *418*, 880–884.

Yuan, A., Dourado, M., Butler, A., Walton, N., Wei, A., and Salkoff, L. (2000). SLO-2, a K^+ channel with an unusual Cl^- dependence. Nat. Neurosci. *3*, 771–779.

Zhang, Z.W., Kaneda, T., Ku, K., Otaki, M., and Oku, H. (2001). Ischemic preconditioning and nicorandil pretreatment improve donor heart preservation. Jpn. Circ. J. *65*, 678–682.